ELSEVIER

Biophysical Chemistry 113 (2005) 41–51

Biophysical Chemistry

www.elsevier.com/locate/bpc

Single-molecule detection of yeast cytochrome *c* by Surface-Enhanced Raman Spectroscopy

Ines Delfino, Anna Rita Bizzarri*, Salvatore Cannistraro

Biophysics and Nanoscience Centre, INFM, Dipartimento Scienze Ambientali-Università della Tuscia, Viterbo 01100, Italia

Received 9 April 2004; received in revised form 7 July 2004; accepted 10 July 2004
Available online 27 September 2004

Abstract

The giant enhancement of Raman signal near silver colloidal nanoparticles is exploited to study the Raman spectrum of Cytochrome *c* from *Saccharomyces cerevisiae* (Yeast Cytochrome *c*—YCc) in the limit of single-molecule. The investigation is performed on proteins both in solution and immobilised onto a glass slide using a quasi resonant laser line as exciting source with low excitation intensity. In both cases, spectra acquired at different times exhibit dramatic temporal fluctuations in both the total spectrum and in the specific line intensity, even though averaging of several individual spectra reproduces the main Raman features of bulk YCc. Analysis of the spectral intensity fluctuations from solutions reveals a multimodal distribution of some specific Raman lines, consistent with the approaching of single molecule regime. Among other results, the statistical analysis of the spectra from immobilised samples seems to indicate dynamical processes involving the reorientational of the heme with respect to the metal surface.

Keywords: Single-molecule; Cytochrome *c*; SERS

1. Introduction

In recent years, the study of proteins in single molecule (SM) regime is attracting increasing interest. The extraordinary development of some optical techniques permitting the detection of specific signal in very low molecule concentration limit [1–6] has opened new opportunities in many disciplines such as biophysics and biomedicine [6]. Measurements on individual molecules have the main advantage of enabling the investigation of phenomena that are usually hidden to ensemble average [7].

Different spectroscopic approaches have so far been applied and developed up to reach single molecule detection, and particular attention has been focused on vibrational spectroscopies [1,2] because they are of fundamental importance for the understanding of internal configurations, structure and dynamics of proteins. In particular, Raman spectroscopy provides significantly a wealth of structural information and can be used to specifically identify molecules with no need of estrinsic labelling of the samples. On the other hand, it generally presents a very low cross-section. The use of a radiation resonant with an electronic transition leads to the Resonance Raman (RR) effect that is characterized by a higher cross section. The finding that Raman signals are enhanced in presence of nanostructured metal surfaces [8] has dramatically boosted Raman spectroscopy as a powerful tool for the vibrational studies in life science in the low concentration limit, because the related cross section can be increased up to a factor 10^{14} [9–11]. The use of silver or gold colloidal nanoparticles to enhance Raman effect on one hand, and the rapidly growing capability (based on advances in both lasers and detectors) to detect very low signals using high-resolution microscopy on the other, has allowed a very wide use of Surface-Enhanced Raman Scattering (SERS) and Surface-Enhanced Resonance Raman Scattering (SERRS) to study the vibrational features of very low concentrated samples, even down

* Corresponding author. Tel.: +39 0761 357027; fax: +39 0761 357119.
E-mail address: bizzarri@unitus.it (A.R. Bizzarri).

0301-4622/$ - see front matter © 2004 Elsevier B.V. All rights reserved.
doi:10.1016/j.bpc.2004.07.006

to single molecule regime [1,2,6,9–13]. This possibility could be particularly appealing in the study of biomolecules, because SM-SERS can be an extraordinary device to go deep inside the functionality and structure of biological proteins also by following an individual molecule throughout the course of events or analyzing the conformational states as function of time.

Recently, a number of works using SERS for the investigation of biomolecules (studies on horseradish peroxidase [15], tyrosine [16], myoglobin [17], haemoglobin [18]) has confirmed such abilities, providing the tool for obtaining very insightful information on a class of biomolecules, the Electron Transfer (ET) proteins, that is attracting much interest from both scientific and bionanotechnological standpoints [19,20]. Their natural redox properties and low dimensions make them good candidates for an integration in hybrid submicrometer-sized electronic components, as well as in novel biosensor configurations [20]. Furthermore, SERS study on ET proteins could give some insights in the explanation of Raman enhancement effect. As a matter of fact, it is acknowledged that two main processes are responsible for Raman enhancement: an electromagnetic effect (EM) and a chemical one that probably involves a charge transfer (CT) between molecule and enhancing surface.

In the main stream of research about ET proteins, we have recently investigated the topological, spectroscopic and electron transfer properties of cytochrome *c* from *Saccharomyces cerevisiae* (Yeast Cytochrome *c*-YCc), directly self-chemisorbed on bare gold electrodes through the free sulfur-containing group [19,21]. YCc is an ET protein having the peculiarity of bearing an additional free sulphur-containing group (Cys102). Thus it results to be highly suitable for specifically oriented interactions with metals with an expected minor perturbation for the heme group and a good electrical contact of YCc with a metal surface. Our results, from Scanning Tunneling Microscopy (STM), Atomic Force Microscopy (AFM) and cyclic voltammetry studies, clearly indicate that this variant of cytochrome *c* is adsorbed on electrodes with preservation of morphological properties and redox functionality showing good coupling with the electrode. To get a deeper insight into charge transfer dynamics and orientation of YCc near a metallic surface, an SM-SERS investigation could be appropriate. Here, we present a preliminary SM-SERS study of YCc, adsorbed on colloidal silver nanoparticles, on both solutions and immobilised samples in order to compare single molecule behavior to the well known average ensemble Raman behavior.

2. Materials and methods

All chemicals ($AgNO_3$, YCc, Trizma, APES) have been purchased from Sigma. Solutions of colloidal silver have been prepared by Lee-Meisel standard citrate reduction method [22]. The concentration of silver particles, estimated by optical absorption, is about 10^{-11} M. AFM studies have revealed that the colloids consist of an heterogeneous size and shape (spheres and rods) particle distribution characterized by an average size of about 70 nm [17].

YCc from *S. cerevisiae* (M.W. 12588 Da) is a small single-domain heme-containing protein, which represents an essential component of the mitochondrial respiratory chain, playing a major role in the ET between two membrane-bound enzyme complexes, cytochrome *c* reductase and cytochrome *c* oxidase. As in many others heme cytochromes, in YCc the heme group is covalently bound to the protein matrix through thioether linkages involving two cysteine residues (Cys14 and Cys17). In addition, YCc bears a free sulphur-containing group (Cys102). YCc solutions, used without further purification, have been prepared dissolving the powder in 1 mM TRIS buffer (pH 8.0) at a concentration of 2.6 mM. Successive dilutions have allowed us to obtain the desired concentrations. For Raman measurements, samples have been prepared at a concentration of 1.6×10^{-4} M YCc, while for SERS measurements an aliquot of a solution has been incubated with colloidal particles for 1 h at room temperature in order to obtain a ratio of 6:1 between the number of colloidal particles and the number of cytochrome molecules at 1.7×10^{-12} M concentration of YCc. SERS measurements on samples in solution have been carried on immediatly after the deposition of a droplet (20 μl) onto a glass slide, previously coated with polymerized 3-aminopropyltriethoxysilane (APES) [23]. Dry samples have been prepared leaving in a dryer for 1 h at room temperature the droplet previously deposited on glass slide.

Raman spectra have been recorded using a Jobin-Yvon Super Labram confocal system equipped with a liquid nitrogen-cooled CCD (EEV CCD10-11 back illuminated; pixel format: 1024×128) detector and a spectrograph with a 1800 g/mm grating allowing a resolution of 5 cm^{-1}. A 100× objective with a numerical aperture N.A.=0.9 has been implemented. The laser source has been an Argon ion laser (MellesGriot) providing a 514.5 nm radiation that is preresonant with the $Q(0,1)$ (520 nm) band, associated with the $Q(0,0)$ band electronic transitions. The provided laser power has been kept below 4 mW (corresponding to about 20 kW/cm^2); 20% of such power really impinging on the sample.

When liquid samples are under investigation, the scattering volume (V_S) can be modelled as a double right cone. From geometrical considerations we have obtained: $V_S=(2\pi/3)\Delta z\cdot(r^2+\omega_0^2+\omega_0 r)$, where Δz=10.7 μm (from technical sheets of the system) is the depth of field, ω_0 is the beam waist of laser ($\omega_0=(4/3)(\lambda/\text{N.A.})$=0.791 μm), r, the spread due to the objective, is $r=\Delta z\cdot\tan(\arcsin(\text{N.A.}/n))$=10 μm, n is the refraction index of the sample, λ is the laser wavelength. In such a way, we have estimated $V_S\approx 2.5$

pl. The average number of investigated particles (N) of a solution with known concentration (c) is connected to the scattering volume, being $N=V_S c N_A$, where N_A is the Avogadro number. In our SERS liquid samples, characterized by $c=1.7\times10^{-12}$ M, the average number of YCc molecules in the scattering volume is 3.

The Raman spectra of high-concentration solutions have been obtained with 10s-integration time. The investigation of SERS liquid and dry samples has been carried on acquiring various time series of spectra with an integration time of 1 s; each spectrum being separated by the successive by 1.4 s.

Since in SM measurements the detected signals are usually very low, the knowledge of the noise of the detector is a crucial point. The total noise (N_t) on a measured intensity acquired with a CCD detector has three components: shot noise (N_{SN}), read out noise (N_R), and dark charge noise (N_D). The combination of these gives the total noise: $N_t=[N_{SB}^2+N_R^2+N_D^2]^{1/2}$. As well known, N_R and N_D are quantified by the chip manifacturer (in our case N_R=6–8 counts for all the chip and N_D=0.1 counts/s for the used chip region, that is 25 x 1024 px), while N_{SN} is given by the square root of the impinging number of photons. Typically in our SM-SERS investigation we have obtained 100–1000 counts (for 1 s integration time) for significant Raman lines, corresponding about to 200–2000 photons as our CCD detector, cooled down to 193 K, has a counting efficiency at the used wavelength of 0.46. In these cases, N_{SN} is of the order of 7–21 counts, and then by neglecting N_D, $N_t=[N_{SN}^2+N_R^2]^{1/2}$ ranging from 13 to 29 counts.

3. Results and discussion

3.1. Raman spectroscopy on bulk samples

The Raman spectrum of YCc bulk solution (1.6×10^{-4} M) is shown in Fig. 1a. This spectrum shows sharp peaks mainly in the region between 1200 and 1700 cm^{-1}. They are associated with the inner and outer ring stretching vibrations of the heme and sensitive to the oxidation, coordination and spin states of the iron. From an analysis of specific Raman lines of Fig. 1a, it comes out that, within the spectral resolution, the positions of the detected peaks are in agreement with those published in literature [24–29] (see Table 1).

Concerning the heme sensitive oxidation modes, from Fig. 1a we note that lines corresponding to ferrous state (ν_{15} at 750 cm^{-1}, and ν_4 at 1363 cm^{-1}) are present. At the same time, lines related to both high spin (HS: ν_{10} at 1621 cm^{-1}) and low spin (LS: ν_{19} at 1584 cm^{-1} and ν_{10} at 1639 cm^{-1}) states can be visualized, even if the intensity of LS marker lines is higher. All the spectral characteristics indicate that the preferred configuration of YCc in solution at a relatively high concentration (1.6×10^{-4} M) and pH 8.0 is a low spin 6 coordinate with reduced iron (usually assumed as native configuration of YCc) even if a slight population of protein with heme in HS configuration is also present consistently with previous studies [27,28]. In addition, we note an intense continuum signal, likely due to incoherently broadened resonance fluorescence associated with Q-band excitation [30], underlying the spectrum.

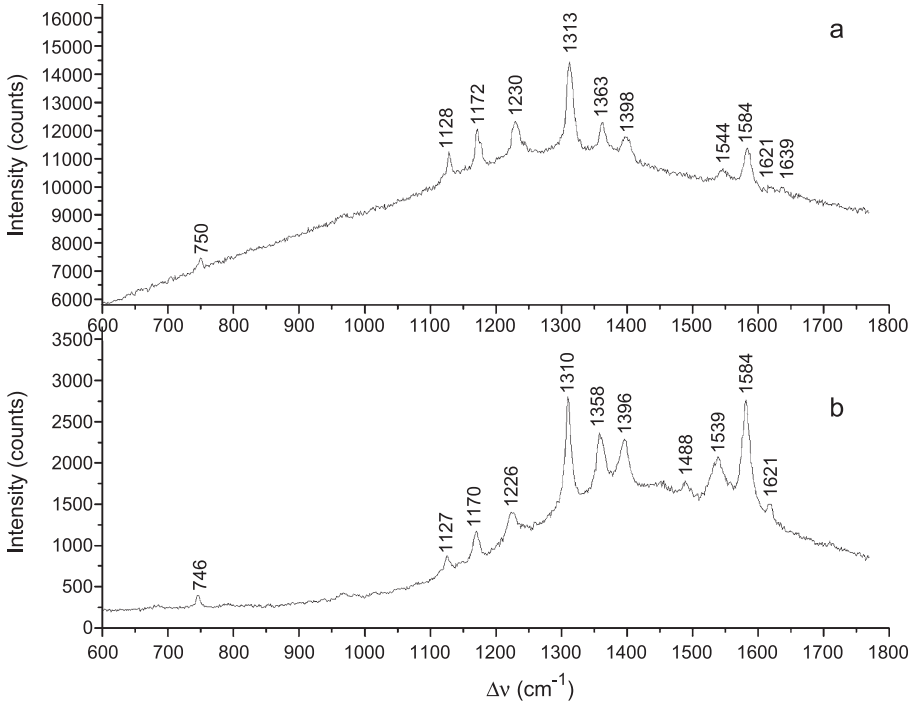

Fig. 1. Raman spectra of 1.6×10^{-4} M-YCc samples at pH 8 with an integration time of 10 s for (a) liquid sample and (b) dry sample. The frequencies of the main peaks are labelled. For details see Table 1.

Table 1
Some Raman frequencies assigned to cytochrome in literature

$\Delta\nu$ (cm^{-1})	Assignment	Mode and Symmetry species
1640	ν_{10} Spin state marker band: low spin [25]	$\nu(C_\alpha C_m)_{asym}$, $B_{1\ g}$
1626	ν_{10} Spin state marker band: high spin [24]	$\nu(C_\alpha C_m)_{asym}$, $B_{1\ g}$
1605	ν_{10} [28]	$\nu(C_\alpha C_m)_{asym}$, $B_{1\ g}$
1587	ν_{19} Spin state marker band: low spin [25]	$\nu(C_\alpha C_m)_{asym}$, $A_{2\ g}$
1568	ν_{19} Spin state marker band: high spin [25]	$\nu(C_\alpha C_m)_{asym}$, $A_{2\ g}$
1540	ν_{11} [26] ν_3 Spin state marker band: high spin [26,28],	$\nu(C_\beta C_\beta)$, $B_{1\ g}$
1501	Oxidation state marker: oxidised (reduced: 1492 cm^{-1}) [26]	$\nu(C_\alpha C_m)$, $A_{1\ g}$
1408	ν_{29} [25,29]	ν(pyr quarter-ring), $B_{2\ g}$
1400	ν_{20} [24]	ν(pyr quarter-ring), $A_{2\ g}$
1375	ν_4 Heme oxidation state marker: oxidised (reduced: 1360 cm^{-1}) [25,29]	$\nu(\text{pyr half-ring})_{sym}$, $A_{1\ g}$
1314	ν_{21} [24]	$\delta(C_mH)$, $A_{2\ g}$
1232	ν_{13} [24]	$\delta(C_mH)$, $B_{1\ g}$
1174	ν_{30} [24]	$\nu(\text{pyr half-ring})_{sym}$, $B_{2\ g}$
1130	ν_{22} [24]	$\nu(\text{pyr half-ring})_{sym}$, $A_{2\ g}$
804	ν_6 [24]	ν(pyr breathing), $A_{1\ g}$
750	ν_{15} [24], reduced iron [28]	ν(pyr breathing), $B_{1\ g}$
674	ν_7 [24]	$\nu(\text{pyr deform})_{sym}$, $A_{1\ g}$

Mode and symmetry species together with expected values of Raman shifts for each lines.

The Raman spectrum of dry YCc samples, shown in Fig. 1b, reveals spectral features quite similar to those of YCc solutions even if a small frequency shift of some lines is detected. Again, the presence of Raman lines located at 1358 and at 1584 cm^{-1} indicates that most of the cytochrome molecules are in LS reduced state. Furthermore, the spectrum of dry YCc samples shows an additional Raman line located at 1488 cm^{-1} which can be assigned to the in plane vibrational modes of $C_\alpha C_m$ bond, ν_3, with the iron in a ferric state [28]. The increase in the intensity of the ν_{10} HS marker (1621 cm^{-1}) suggests a higher number of molecules having a heme in HS configuration with respect to liquid samples. Remarkably, the continuum signal is much reduced with respect to spectrum in solution (Fig. 1a) suggesting a dependence of the fluorescence signal from the water content of the samples.

3.2. SERS measurements on solutions

Investigation of low concentrated (1.7×10^{-12} M) YCc solutions has to be carried on in the presence of silver colloids in order to enhance Raman signal that otherwise is negligible at similar concentrations. Series of 1800, 1-s integration time SERS spectra, lasting 1.4 s between two successive measurements have been acquired to get temporal information about SERS signals. These spectra are characterized by dramatic temporal fluctuations in the intensity of some lines (see as examples the spectra shown in Fig. 2). In general, a marked variability in the signal intensity appears in SM-spectroscopy and it is considered as an hallmark of single-molecule regime [6]. In the present case, the strong intensity fluctuations of the Raman signals, and the feature that only a subset of the Raman peaks of the protein under study are detected, are reminiscent of the behaviour reported in literature about SM-SERS measurements [13,14,17,18].

It should be noted that when all the spectra of a series are summed up, almost all the vibrational features of the bulk YCc are recovered, as shown in Fig. 3, even if there are some differences as discussed below. Two additional lines (located at 804 and 674 cm^{-1}) due to pyrrole breathing and pyrrole deformations have been detected together with a small frequency shift for quite all the lines, as often happens in SERS measurements [9]. However, the absence of a significative shift of specific Raman lines (ν_{19} mode, as an example) sensitive to protein denaturation and partial unfolding [25] suggests that the YCc has preserved its native structure.

From the analysis of Raman lines, it emerges that both HS state (line at 1622 cm^{-1}) and LS state (line at 1584 cm^{-1}) heme are present also in this case. Some lines are probably partially masked in the average spectrum by other Raman features due to YCc and/or to impurities. As the oxidation state of the iron is concerned, indication of both Fe^{2+} and Fe^{3+} states are detected: the significative downshift of bands due to ν_{20} mode to 1391 cm^{-1}, and the sharp peak at 1360 cm^{-1} are related to the presence of reduced iron, while the lines at 1498 and 1622 cm^{-1} indicate that at least a portion of the investigated molecules is in the HS oxidised state also in dry samples [25,26].

Notably, the continuum signal due to non-specific fluorescence has disappeared. This can be attributed to the fluorescence quenching effect of the colloids [31] that is one of the main characteristics of SERS experiments. Actually, the quenching effect of a noble metallic surface enables to extend Raman spectroscopy to molecules having very high fluorescence signal that can be suppressed in SERS measurements.

It should be noted that two large symmetrical peaks positioned around at 1350 and 1595 cm^{-1} underlining the average spectrum can be observed. These peaks have been also detected in the Raman spectrum of the bulk Ag nanoparticle solution. Their presence is well known in literature and can be ascribed, according to Ref. [32], to carbon contaminations due to particles passing in the scattering volume during the measurements.

Although strong fluctuations in the Raman intensity could be considered peculiar of SM regime, we have submitted our data to a statistical analysis to ascertain if they meet the evaluation criteria currently accepted as indicative of SM regime [13]. Accordingly, the intensity distribution of relevant Raman lines which represent a

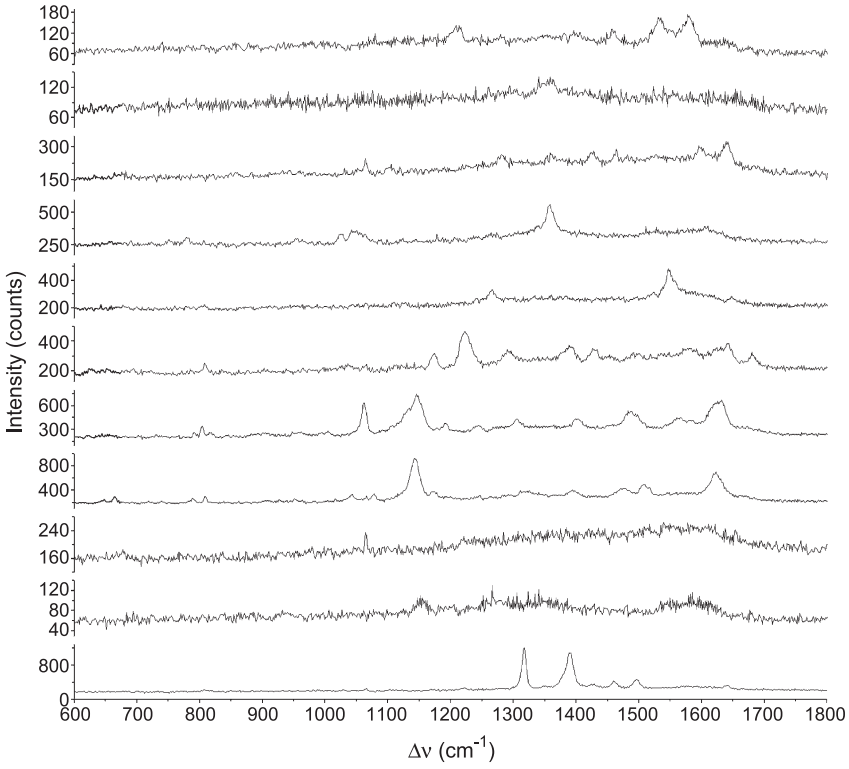

Fig. 2. Selected SERS spectra from series acquired from 1.7×10^{-12} M YCc solution with Ag-colloids. The scaling of every spectrum is different in order to evidence the features of each spectrum.

fingerprint of the molecule under investigation has been analyzed. We have selected, among the 1800 spectra of the series, those spectra with Raman lines featuring an average intensity higher than the signal from the colloidal particles (whose mean value is estimated to be 18 counts; inset of Fig. 4). The other spectra have been analysed in order to define the mean Raman signal detected when no YCc molecules are in the scattering volume; this value being considered as zero-distribution. On such a ground, 140

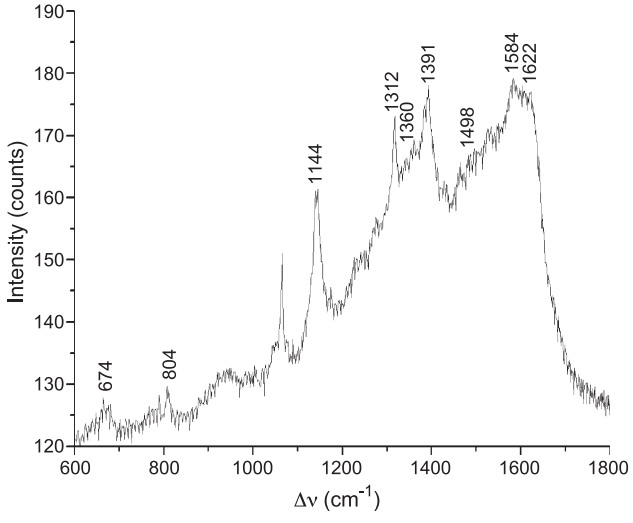

Fig. 3. SERS spectrum averaged over all the 1800 spectra of the series acquired from 1.7×10^{-12} M YCc solution with Ag-colloids. The frequencies of the main peaks are labelled.

spectra over 1800 having been sorted. This means that 8% of spectra have been really enhanced over the total number of spectra acquired in our samples and experimental conditions. This is in agreement with previous reports [13,18] in which the presence of the so-called hot sites has been ascribed to the formation of nanoparticles aggregates which give rise to a huge EM enhancement [33]; these aggregates representing only a few percent of the target molecules. Furthermore, in the hypothesis that the colloidal particle+YCc system in solution is experiencing Brownian motion, an average residence time in the probed volume of 10 s can be roughly estimated [34], in good agreement with previous reports [13]. Since such a value is 10 times longer than the acquisition time of each spectrum, it is likely that each spectrum is generated by the same molecule. The distribution in the intensities of the line at the frequency 1584 cm^{-1} (related to ν_{19} mode) for the 140 selected spectra is shown in Fig. 4. The resulting histogram when the same analysis is performed on 140 spectra from the bare colloidal solution is shown in the inset of Fig. 4. The plot of the occurrence of the selected Raman line intensity of the YCc colloidal solution appears multimodal and a fit (see the continuous line in Fig. 4) of the histogram, with a superposition of three Gaussian curves, indicates the presence of three peaks whose occurrence progressively decreases as long as higher Raman intensities are taken into account. The Gaussian distributions are centred at 73 ± 2, 142 ± 3, 242 ± 11 counts, respectively. Within the errors, equal separations between two successive maxima (about 70

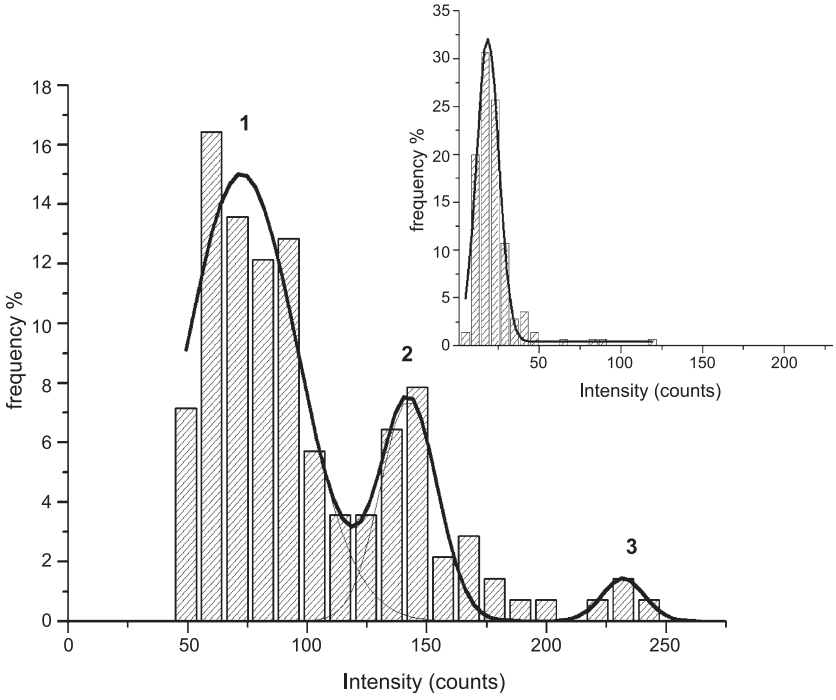

Fig. 4. Statistical analysis for 1584 cm^{-1} line intensity of the 140 selected SERS spectra of 1.7×10^{-12} M YCc solution with Ag-colloids. The origin of the *x*-axis has been fixed at the central value of the intensity distribution of the signal when only colloids are in the scattering volume. The histogram has been obtained using 20 bins whose widths are 5% of maximum intensity. The peaks reflect the probability to find just one, two or three molecules in the scattering volume. Inset: statistical analysis on the intensity at the same Raman frequency (1584 cm^{-1}) measured in 140 spectra related to a solution containing only Ag-colloidal particles.

counts) are observed. A similar behaviour for some other specific Raman line intensities has been also obtained (not shown). Conversely, distribution related to the intensity of the bare colloid solution, shown in the inset of Fig. 4, can be described by only one Gaussian curve centered at 18 counts and wide about 13 counts, in good agreement with what expected from the CCD noise level (about 14 counts). The observed trend shown in Fig. 4 can be interpreted in terms of detection of a different number of hot SERS centres during the measurements. In particular, as due to diffusion of metal particles, 1, 2, and 3 emitting SERS hot sites can be found in the scattering volume; the occurrence, and hence, the probability, of finding a higher number of hot emitting particles progressively decreases. The experimental evidence that the Raman intensity distributions are substantially equispaced is consistent with such a hypothesys. Such a result finds a close correspondence with that occurring for crystal violet and myoglobin silver colloid samples in the single molecule limit [13,17].

In summary, our data about YCc silver particle solutions point out a marked deviation from a single mode distribution and a large spread for the line intensity of YCc colloidal solution at a concentration of 1.7×10^{-12} M. These findings, in agreement with what was observed in Refs. [13,17], suggest that in our measurements, SERS signals from single molecules have been detected. It should be pointed out that, even if more than one YCc molecule are expected to be present in the scattering volume, the restrictive conditions required to obtain large enhanced Raman signals are satisfied only for a small portion of molecules.

3.3. SERS measurements on immobilised samples

In principle, the detection of signals in the single molecule limit could offer the exciting possibility of investigating whether the vibrational features of a single YCc protein molecule deviate from those of the ensemble. However, the diffusion-based selection of the molecule when solutions are under investigation means that different molecules are studied during the course of the experiment (due to molecules entering and leaving the scattering volume). Therefore, the actual time evolution of a specific single molecule cannot be followed. In this respect, a more convenient approach might be represented by the study of immobilized particles. So, to follow the dynamics of single YCc molecule for long periods, SERS measurements as a function of time of immobilised Ag nanoparticles with 1.7×10^{-12} M YCc have been performed.

We have identified Raman scattering sites by manually scanning (on *x*–*y* plane) the sample under the microscope objective and locating brightly emitting colloidal particles. Highly inhomogeneous Raman intensity over individual hot spots has been found consistently with what usually reported in SM-SERS about immobilised particles [14,35]. We have focused our attention on those active sites having the lowest Raman intensity, among the ones showing YCc

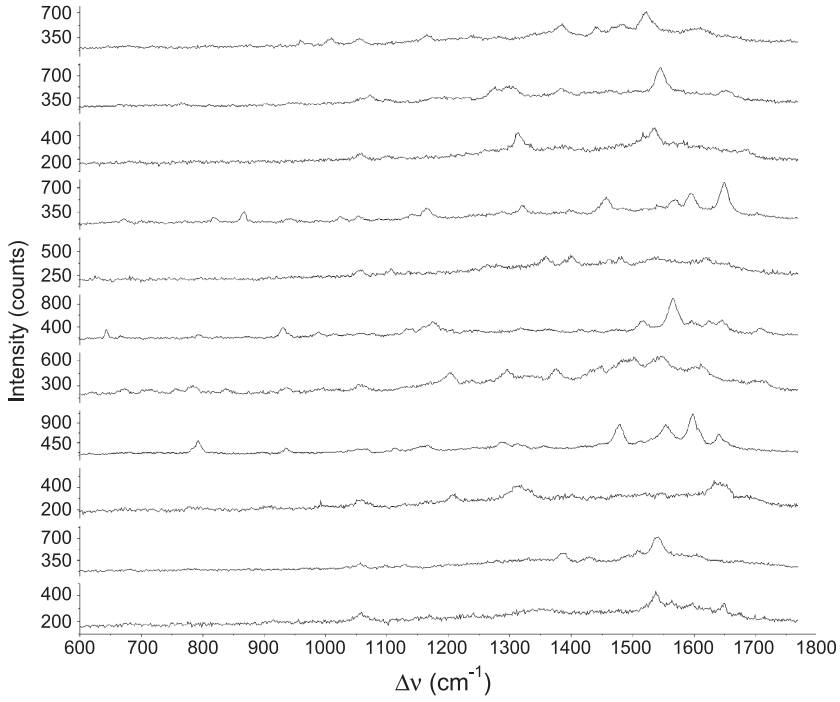

Fig. 5. SERS spectra selected within a temporal series from a bright site of immobilised Ag-colloids incubated with YCc at a concentration of 1.7×10^{-12} M. The scaling of every spectrum is different in order to evidence the features of each spectrum.

specific vibrational features. For a selected site, series of 500 1s-integration time spectra have been acquired. Recorded Raman signals fluctuate in time as shown in Fig. 5, where some spectra of a series are reported as specimens. Also in this case variation in peak intensity and/or frequency changes of some Raman lines are detected. Furthermore, the spectrum of the free heme has never been recorded in our series of measurements; this being a support for assessing that the spectra are from YCc-bound heme. Again, when all the spectra of a series are summed up, the resulting spectrum exhibits Raman features similar to those of bulk dry YCc spectrum (see Fig. 6). The evidence that the

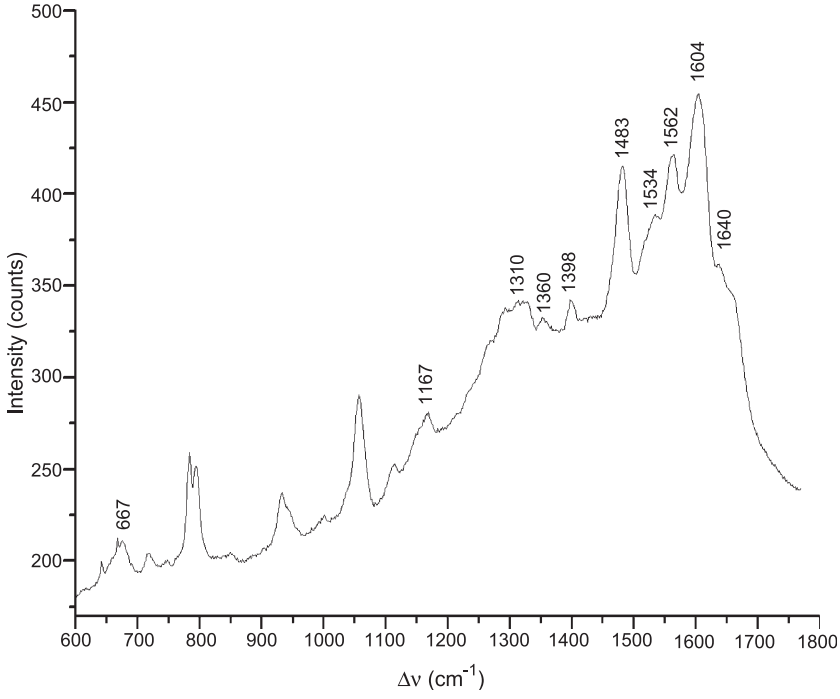

Fig. 6. SERS spectrum averaged over all the 500 spectra of a selected series acquired from a bright site of immobilised Ag-colloids incubated with YCc at a concentration of 1.7×10^{-12} M. The frequencies of the main peaks are labelled.

vibrational features of the ensemble-averaged spectra can be reproduced suggests an ergodic behaviour of the sample, consistently with what was recently verified for other small molecules [14]. An analysis of the spectrum shown in Fig. 6 reveals a shift in some frequencies. In particular, the downshift of the line due to ν_3 mode to 1483 cm^{-1} and of the peak related to ν_{10} mode to 1604 cm^{-1} can be connected to 5cHS configuration [28] assumed by the heme at some times. However, the picture of the sample depicted from the time-average spectrum is that also in this case there are populations of molecules characterized by HS (ν_3 mode located at 1483 cm^{-1}, ν_{10} at 1604 and 1640 cm^{-1}) and LS (ν_{19} at 1562 cm^{-1}) heme configurations and that the iron is mainly present in ferrous (ν_4 at 1360 cm^{-1} and ν_{10} at 1604 cm^{-1}) state. Notably, there are some differences between spectra of YCc Ag-colloidal samples in solution and immobilised onto a glass slide (Figs. 3 and 6); such differences could be explained by taking into account for the effects induced by the water presence on both protein configurations and protein–metal interaction [36].

It has been shown that a lot of information about dynamics, orientation and heterogeneity of the molecules is hidden in the temporal fluctuations of Raman signal of single molecule (or a few molecules). Actually, effects connected to entanglement and/or gating of modes or to the environmental changes [14] can be put out. Usually, to disclose such information, a detailed analysis of temporal fluctuations of some lines characteristic of the investigated molecule is carried on. In the present case, we focus our attention on the temporal evolution of three peculiar frequencies (1360, 1408, and 1626 cm^{-1}; some of them, partially masked in the average spectrum, having been clearly detected in many of the spectra in the selected temporal series) and of the average spectrum intensity. The temporal trends of the intensity of such Raman lines and of the average spectrum intensity, together with the related intensity distributions, are shown in Fig. 7. Regarding the temporal trends, we note that at some times the lines undergo intensity jumps. Some of these jumps appear at the same times in the different lines and in the average spectrum intensity. The related intensity histograms can be described by only a single mode distribution with similar central values but different widths. Differences (from a minimum of 200 counts up to

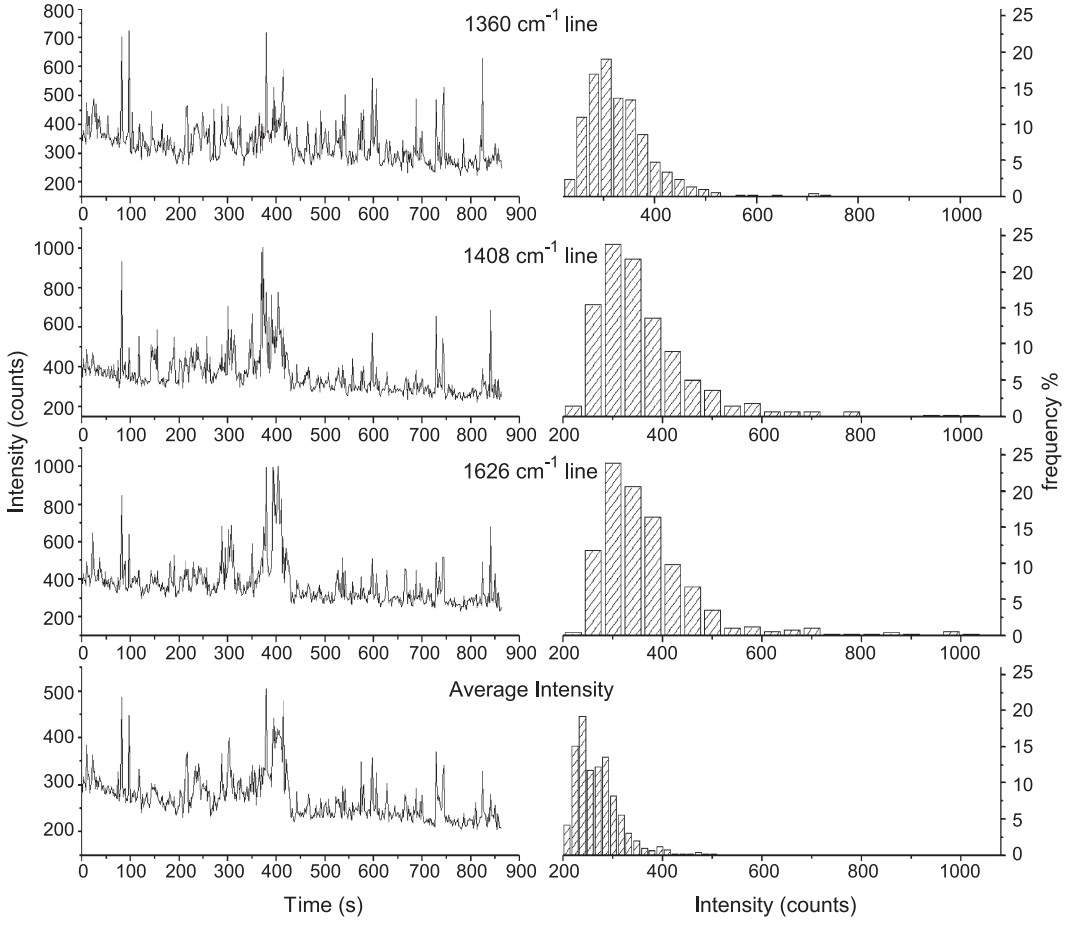

Fig. 7. Temporal trend of SERS intensity and related distribution for different frequencies of the selected series obtained from a bright site of immobilised Ag-colloids incubated with YCc at a concentration of 1.7×10^{-12} M. The average intensity has been calculated by averaging the detected intensity of each spectrum over the frequencies. The histograms have been obtained by using 20 bins whose widths are 5% of maximum intensity. No background subtraction has been carried on.

1250 counts) are indicative of the specificity in the temporal behaviour of the various vibrational modes. Distribution widths can be estimated to be in the order of 80–200 counts, significantly higher than that expected from detector noise (14 counts) or from the signals of silver nanoparticles (18 counts). This means that the intensity fluctuations, resulting in the great enlargement of intensity distributions, cannot be connected only to the noise or to the presence of colloids, suggesting that some other effects, spontaneous or photoinduced [35], should be involved. These results are in agreement with those recently reported for protoporphyrin and myoglobin molecules [14,17] and they may be generally related to the broadening of specific Raman lines as due to superposition of processes inducing Raman signals in the same frequency region. Indeed, in Raman experiments on bulk samples, the inhomogeneous line broadening usually observed can be described in terms of superposition of signals arising from a variety of molecules arranged in different conformational substates [37], or related to averaged properties over a heterogeneous population of molecules. The point of view of experiments about a single molecule (or few molecules) is really different because such measurements enable to follow the temporal behaviour of individual molecules. In this frame, the broadening of intensity distributions could be attributed to enlargement of specific Raman lines due to the sampling of different conformational substates that the system experiences in time. The dynamical processes are influenced by an extensive coupling of the active Raman sites to the overall dynamics of the protein [37,38].

Therefore, various effects are governing the temporal behaviour of Raman signal. Often, the study of the relative intensity of specific lines is employed to disclose the information embedded in the temporal trends of Raman lines [26,29,39]. In the case of YCc, there are intensity ratios particularly interesting as they are sensitive to the orientation of the heme with respect to the metallic surface. We have analysed the following extracted: (a) intensity ratio of lines located at 1626 cm^{-1} and at 1360 cm^{-1} ($R_a=I_{1626}/I_{1360}$), (b) intensity ratio of lines located at 1408 cm^{-1} and at 1626 cm^{-1} ($R_b=I_{1408}/I_{1626}$). To get rid of effects due to noise fluctuations, we investigate the time-dependent temporal behaviour of the fractional value ($\delta R/\langle R\rangle=(R(t)-\langle R\rangle)/\langle R\rangle$) of each of the two ratios [39]. These trends are shown in Fig. 8 together with the relative variation of the average spectrum intensity. The ratio variations are in the order of 10–40%, while the average spectrum intensity variations are even higher (up to 400%). The richness of features in the time trajectory of the average intensity (Fig. 8c) suggests that a variety of processes are

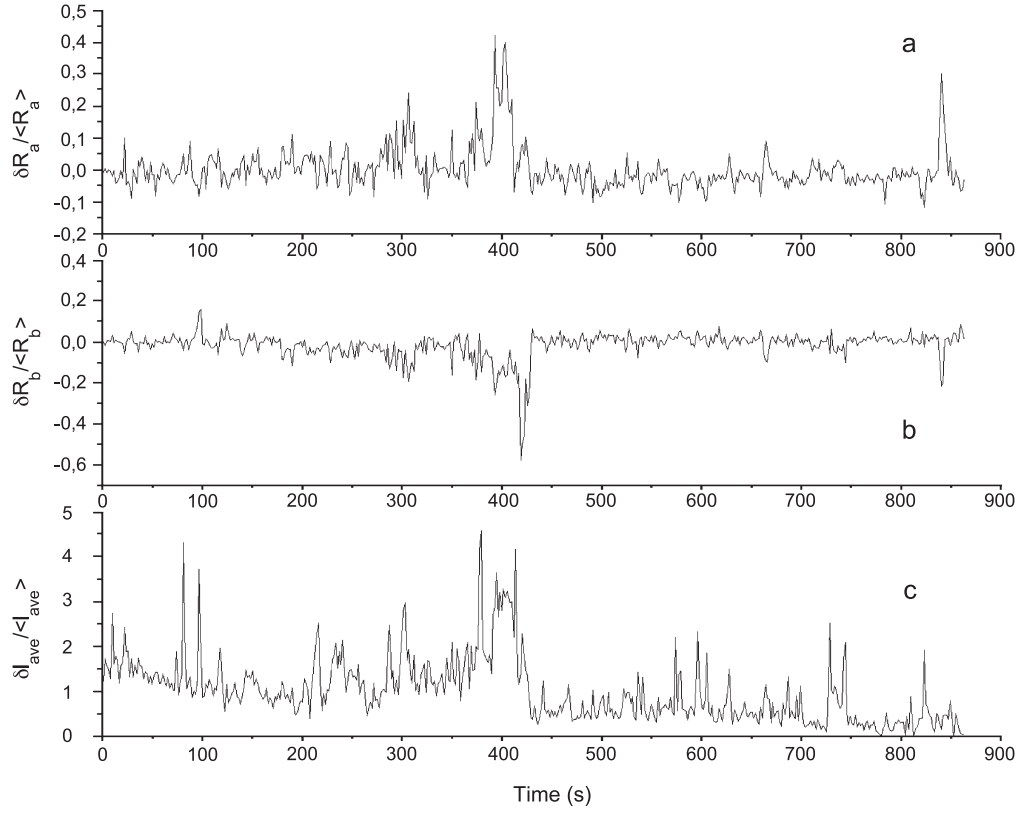

Fig. 8. Temporal trend of ratios between vibrational band intensities in the SERS spectrum of a single YCc molecule immobilised on Ag-colloids, presented as fractional fluctuations from the mean, (($\delta R/\langle R\rangle$)=(($R(t)$-$\langle R\rangle$)/$\langle R\rangle$)). (a) $R_a=I_{1626}/I_{1360}$, (b) $R_a=I_{1408}/I_{1626}$, (c) fluctuations from the intensity averaged over all the frequencies.

governing the fluctuation of Raman signal. Actually, the overall intensity is sometimes related to many physical/chemical processes, such as electron transfer between protein and substrate and the intrinsic dynamics of the target molecule [14,40].

Notably, most times a positive jump in δR_a corresponds to a negative jump in δR_b and a positive jump in the average intensity. This is consistent with a change in the orientation of the protein respect to the enhancing surface if one considers the symmetry properties of Raman active modes assigned to the selected lines; being mode ν_4 (line at 1360 cm^{-1}) totally symmetric, and mode ν_{10} (line at 1626 cm^{-1}) non totally symmetric. For a heme cromophore having a symmetry of D_{4h}, that is the typical model used to describe a cytochrome *c* heme [24,25], both Raman signals due to totally symmetric modes (e.g., $A_{1\ g}$ mode ν_4, 1360 cm^{-1}) and non totally symmetric modes (e.g., $B_{1\ g}$ mode ν_{10}, 1626 cm^{-1}) involve motions along the *x*- and *y*-axes (in the plane of the porphyrin), while the totally symmetric modes involve displacements along the *x*, *y*, and *z* directions. The SERS effect preferentially enhances vibrations which involve a change in polarizability along an axis perpendicular to the surface [29]. Thus, the non-totally symmetric modes would be enhanced only when the heme in-plane vibrations have a large component perpendicular to enhancing surface. At variance, when the heme plane lies parallel to the surface only Raman scattering of totally symmetric modes is enhanced. Thus, when the angle of the heme with respect to the surface normal increases, a relative increase in SERS intensity for nontotally symmetric modes over totally symmetric modes is predicted. On such a ground, an increasing of Raman signal of ν_{10} with respect to the one due to ν_4 suggests a reorientation of the heme ring to an increased angular position relative to the metal surface plane. Confirmation of a more vertical inclining prosthetic group comes from the reduced intensity of ν_{29} ($B_{2\ g}$, 1408 cm^{-1}) relative to ν_{10} [25], that is a relative decreasing of δR_b. Such motion probably influences all the protein, inducing a reorganization of the YCc depending on the heme position.

4. Conclusions

SERS technique enables the investigation of the vibrational modes of YCc, a molecule which deserves some biotechnological interest, at very low concentrations. The goal is achieved by exploiting the huge enhancement effect of the Raman cross section by adsorbing the protein on silver nanoparticles in both solution and immobilised on a glass surface. In liquid samples, the statistical analysis allows us to distinguish different discrete populations of molecules and to assess that the single molecule regime is approached. In dry samples, where we get rid of effects due to Brownian motions of molecules, the temporal behaviour of some specific intensity ratios put into evidence some dynamical effects. Among the ones affecting the investigated time trajectories, we extract, by means of symmetry considerations, some processes that appear to be connected to reorientational events of the YCc-bound heme with respect to the enhancing metal surface.

Acknowledgments

This work has been partially supported by the FIRB-MIUR Project Molecular Nanodevices and by the EC Project SAMBA (V Frame FET).

References

[1] S. Nie, S.R. Emory, Probing single molecules and single nanoparticles by surface-enhanced Raman scattering, Science 275 (1997) 1102–1106.
[2] K. Kneipp, H. Kneipp, I. Itzkan, R.R. Dasari, M.S. Feld, Ultrasensitive chemical analysis by Raman spectroscopy, Chem. Rev. 99 (1999) 2957–2976.
[3] N.F. van Hulst, J.A. Veerman, M.F. Garcia-Parajo, L. Kuipers, Analysis of individual (macro)molecules and proteins using near-field optics, J. Chem. Phys. 112 (2000) 7799–7810.
[4] T. Baschè, W.E. Moerner, M. Orritt, U.P. Wild (Eds.), Single-Molecule Optical Detection, Imaging and Spectroscopy, VCH, Germany, 1997.
[5] Z.J. Donhauser, B.A. Mantooth, K.F. Kelly, L.A. Bumm, J.D. Monnell, J.J. Stapleton, D.W. Price Jr., D.L. Allara, J.M. Tour, P.S. Weiss, Conductance switching in single molecules through conformational changes, Science 292 (2001) 2303–2307.
[6] W.E. Moerner, A dozen years of single-molecule spectroscopy in physics, chemistry, and biophysics, J. Phys. Chem., B 106 (2002) 910–927.
[7] J.A. Veerman, M.F. Garcia-Parajo, L. Kuipers, N.F. van Hulst, Time-varying triplet state lifetimes of single molecules, Phys. Rev. Lett. 83 (1999) 2155–2158.
[8] M. Fleischman, P.J. Hendra, A.J. McQuillan, Raman spectra of pyridine adsorbed at a silver electrode, Chem. Phys. Lett. 26 (1974) 163–166.
[9] K. Kneipp, H. Kneipp, I. Itzkan, R.R. Dasari, M.S. Feld, Surface-enhanced Raman scattering and biophysics, J. Phys., Condens. Matt. 14 (2002) R597–R624.
[10] K. Kneipp, H. Kneipp, I. Itzkan, R.R. Dasari, M.S. Feld, Surface-enhanced Raman scattering: a new tool for biomedical spectroscopy, Cur. Sci. 77 (1999) 915–924.
[11] H. Xu, J. Aizpurua, M. Käll, P. Apell, Electromagnetic contributions to single-molecule sensitivity in surface-enhanced Raman scattering, Phys. Rev., E 62 (2000) 4318–4324;
P. Etchegoing, H. Liem, R.C. Maher, L.F. Cohen, R.J.C. Brown, H. Hartigan, M.J.T. Milton, J.C. Gallop, A novel amplification mechanism for surface-enhanced Raman scattering, Chem. Phys. Lett. 366 (2002) 115–121.
[12] T.M. Cotton, J.-H. Kim, G.D. Chumanov, Application of surface-enhanced Raman spectroscopy to biological systems, J. Raman Spectrosc. 22 (1991) 729–742.
[13] K. Kneipp, Y. Wang, H. Kneipp, L.T. Perelman, I. Itzkan, R.R. Dasari, M.S. Feld, Single molecule detection using surface-enhanced Raman scattering (SERS), Phys. Rev. Lett. 78 (1997) 1667–1670.
[14] A.R. Bizzarri, S. Cannistraro, Temporal fluctuations in the SERRS spectra of single iron-protoporphyrin IX molecule, Chem. Phys. 290 (2003) 297–306.

[15] E.J. Bjerneld, Z. Földes-Papp, M. Käll, R. Rigler, Single-molecule surface-enhanced Raman and fluorescence correlation spectroscopy of horseradisch peroxidase, J. Phys. Chem., B 106 (2002) 1213–1218.
[16] E.J. Bjerneld, P. Johansson, M. Käll, Single molecule vibrational fine-structure of tyrosine adsorbed on Ag nano-crystals, Single Mol. 1 (3) (2000) 239–248.
[17] A.R. Bizzarri, S. Cannistraro, Surface-enhanced resonance Raman spectroscopy signals from single myoglobin molecules, Appl. Spectrosc. 56 (2002) 1531–1537.
[18] H. Xu, E.J. Bjerneld, M. Käll, L. Börjesson, Spectroscopy of single hemoglobin molecules by Surface Enhanced Raman Scattering, Phys. Rev. Lett. 83 (1999) 4357–4360.
[19] A.G. Hansen, A. Boisen, J.U. Nielsen, H. Wackerbarth, I. Chorkendorff, J.E.T. Andersen, J. Zhang, J. Ulstrup, Adsorption and interfacial electron transfer of *Saccharomyces cerevisiae* yeast cytochrome *c* monolayers on Au(111) electrodes, Langmuir 19 (2003) 3419–3427.
[20] J. Willner, Biomaterials for sensors, fuel cells, and circuitry, Science 298 (2002) 2407–2408;
C. Joachim, J.K. Ginzewski, A. Aviram, Electronics using hybrid-molecular and mono-molecular devices, Nature 408 (2000) 541–548.
[21] B. Bonanni, D. Alliata, A.R. Bizzarri, S. Cannistraro, Topological and electron transfer properties of yeast cytochrome *c* adsorbed on bare gold electrode, Chem. Phys. Chem. 4 (2003) 1183–1188.
[22] P.C. Lee, D. Meisel, Adsorption and surface-enhanced Raman of dyes on silver and gold sols, J. Phys. Chem. 86 (1982) 3391–3395.
[23] R.G. Freeman, K.C. Grabar, K.J. Allison, R.M. Bright, J.A. Davis, A.P. Guthrie, M.B. Hommer, M.A. Jackson, P.C. Smith, D.G. Walter, M.J. Natan, Self-assembled metal colloid monolayers—an approach to SERS substrates, Science 267 (1995) 1629–1632.
[24] S. Hu, I.K. Morris, J.P. Singh, K.M. Smith, T.G. Spiro, Complete assignment of cytochrome *c* Resonance Raman spectra via enzymathic reconstitution with isotopically labeled hemes, J. Am. Chem. Soc. 115 (1993) 12446–12458.
[25] I.D.G. Macdonald, W.E. Smith, Orientation of cytochrome *c* adsorbed on a citrate-reduced Silver colloid surface, Langmuir 12 (1996) 706–713.
[26] L.H. Eng, V. Schlegel, D. Wang, H.Y. Neujahr, M.T. Stankovich, T. Cotton, Resonance Raman scattering and surface-enhanced resonance Raman scattering studies of oxido-reduction of cytocrhome c3, Langmuir 12 (1996) 3055–3059.
[27] H. Wackerbarth, P. Hildebrandt, Redox and conformational equilibria and dynamics of cytochrome *c* at high electric fields, Chem. Phys. Chem. 4 (2003) 714–724.
[28] S. Oellerich, H. Wackerbarth, P. Hildebrandt, Spectroscopic characterization of nonnative conformational states of cytochrome *c*, J. Phys. Chem., B 106 (2002) 6566–6580.
[29] C.D. Keating, K.M. Kovalewski, M.J. Natan, Protein:colloid conjugates for surface enhanced Raman scattering: stability and control of protein orientation, J. Phys. Chem., B 102 (1998) 9404–9413.
[30] J.M. Friedman, D.L. Rousseau, Simultaneous observation of coherent and incoherent resonant re-emission in the condensed phase, Chem. Phys. Lett. 55 (1978) 488–492.
[31] T. Pal, N.R. Jana, T. Sau, Nanoparticle induced fluorescence quenching, Radiat. Phys. Chem. 1 (1997) 127–130.
[32] A. Otto, What is observed in single molecule SERS, and why? J. Raman Spectrosc. 33 (2002) 593–598.
[33] Z. Wag, S. Pan, T.D. Krauss, H. Du, L.J. Rothberg, The structural basis for giant enhancement enabling single-molecule Raman scattering, Proc. Natl. Acad. Sci. U. S. A. 100 (2003) 8636–8643.
[34] Resident time (t_d) has been evaluated consistently with Ref. [13]: $t_d=(w^2)/(2D)$, where w is the radius of the volume and D the diffusion coefficient of colloidal particles; w has been estimated by geometrical consideration involving the scattering volume (that is a double right cone) to be in the order of 5–6 μm; D is in the order of 10^{-8} cm^2/s applying Stokes-Einstein relation, $D=(k_BT)/(6\pi\eta r)$, to spherical particles (Ag nanoparticles) with r=40 nm diffusing in water.
[35] Y.D. Suh, G.K. Schenter, L. Zhu, H.P. Lu, Probing nanoscale surface enhanced Raman-scattering fluctuation dynamics using correlated AFM and confocal ultramicroscopy, Ultramicroscopy 97 (2003) 89–102.
[36] G. Smulevich, T.G. Spiro, Surface enhanced Raman spectroscopic evidence that adsorption on silver particle can denature heme proteins, J. Phys. Chem. 89 (1985) 5168–5173.
[37] M.A. Webb, C.M. Kwong, G.R. Loppnow, Excited-state charge-transfer dynamics of azurin, a blue copper protein, from resonance Raman intensities, J. Phys. Chem., B 101 (1997) 5062–5069.
[38] E. Fraga, M.A. Webb, G.R. Loppnow, Charge-transfer dynamics in plastocyanin, a blue copper protein, from resonance Raman intensities, J. Phys. Chem. 100 (1996) 3278–3287.
[39] A. Weiss, G. Haran, Time-dependent single-molecule Raman scattering as a probe of surface dynamics, J. Phys. Chem., B 105 (2001) 12348–12354.
[40] A.M. Michaels, M. Nirmal, L.E. Brus, Surface enhanced Raman spectroscopy of individual rhodamine 6G molecules on large Ag nanocrystals, J. Am. Chem. Soc. 121 (1999) 9932–9939.